JOURNAL OF GEOPHYSICAL RESEARCH, VOL. 104, NO. B2, PAGES 2875–2893, FEBRUARY 10, 1999

Spatial distribution of hotspot material added to the lithosphere under La Réunion, from wide-angle seismic data

Philippe Charvis,[1] Agus Laesanpura,[1] Josep Gallart,[2] Alfred Hirn,[3] Jean-Claude Lépine,[3] Béatrice de Voogd,[4] Tim A Minshull,[5] Yann Hello,[1] and Bernard Pontoise[1]

Abstract. Wide-angle seismic lines recorded by ocean bottom and land seismometers provide a pseudo three-dimensional investigation of the crust and upper mantle structure around the volcanically active hotspot island of La Réunion. The submarine part of the edifice has fairly low seismic velocities, without evidence for intrusives. An upper unit with a velocity-depth gradient is interpreted as made of material erupted subaerially then transported and compacted downslope. Between this unit and the top of the oceanic plate, imaged by normal incidence seismic reflection, a more homogeneous unit indicated by shadow zones on several wide-angle sections may correspond to lavas of a different nature, extruded underwater in the earlier phase of volcanism. Coincident wide angle and normal incidence reflections document that the oceanic plate is not generally downwarping toward the island but doming instead toward its southeastern part, with limited evidence for some intracrustal intrusion. Deeper in the lithosphere, the presence of a layer of intermediate velocity between the crust and mantle is firmly established. It is interpreted as resulting from the advection of hotspot magmatic products, possibly partially molten, and of a composition for which the crust is a density barrier. The extensive wide-angle coverage constrains the extent of this body. It does not show the elongated shape expected from plate drift above a steady hotspot supply. Alternative propositions can hence be considered, for example, that La Réunion is caused by a solitary wave of hotspot material or by a young hotspot. The size of the underplate, 140 km wide and up to 3 km thick, corresponds to less than half the volume of the edifice on top of the plate.

1. Introduction

The origin and evolution of La Réunion and its active volcano, Piton de la Fournaise, are due to the interaction of a mantle plume with the lithosphere. The oldest volcanic rocks known at Réunion are 2.1 m.y. old [*Mc Dougall*, 1971] but the volcanism possibly started as soon as 5 m.y. ago [*Upton*, 1982]. Island of La Réunion lies at the southernmost end of the Mascarene Ridge, a NNE-SSW topographic high (Figure 1), which is usually interpreted as the track of the Réunion hotspot on the African Plate. Magmatic processes build the volcanic edifice itself but may also add material to the lithosphere beneath it. Magmatic material underplated at the base of the crust was inferred from seismic data beneath the older part of the Hawaiian volcanic chain [*ten Brink and Brocher*, 1987] and beneath the 1 to 6 m.y. old Marquesas Archipelago [*Caress et al.*, 1995].

[1]Unité Mixte de Recherche Géosciences Azur, Institute Français de Recherche Scientifique pour le Développement en Coopération, Villefranche-sur-mer, France.

[2]Institut de Ciences de la Terra, Consejo Superior de Investigaciones Cientificas, Barcelona, Spain.

[3]Insitut de Physique du Globe de Paris, Laboratoire de Sismologie Expérimentale, UA 195 CNRS, Paris.

[4]Laboratoire de Géophysique and Unité Mixte de Recherche 5831, Pau, France.

[5]Bullard Laboratoires, Department of Earth Sciences, University of Cambridge, Cambridge, England, United Kingdom.

Paper number 98JB02841.
0148-0227/99/98JB-02841$09.00

A two-dimensional wide-angle seismic investigation of the crust and upper mantle along a 250 km long transect (labeled R4 and R23, Figure 2) parallel to the NE-SW track of the Réunion hotspot provides evidence for an intermediate layer between normal crust and mantle beneath the southwestern half of the Réunion edifice and constrains processes of magmatic discharge of the mantle plume along the hotspot track [*Gallart et al.*, this issue]. A network of multichannel seismic (MCS) profiles strongly suggests that the top of the preexisting oceanic plate is not depressed in the vicinity of La Réunion and may even locally rise islandward [*de Voogd et al.*, this issue].

In this paper, based on the interpretation of wide-angle seismic data recorded at sea, using ocean bottom seismometers (OBS), and on the island using land seismometers (LS), we attempt to map the topography of the oceanic basement and of the Moho beneath the volcanic edifice and to evaluate the regional extent of the crust-mantle intermediate layer using wide-angle seismic lines R24, R18, and R12 (Figure 2). This pseudo 3-D investigation provides an estimate of the volumes involved in the different parts of the structure.

2. Data Processing and Interpretation

Two sets of wide-angle seismic lines were recorded together with coincident MCS lines in August 1993 around La Réunion during cruise 76 of the R/V *Marion Dufresne*. Radial marine profiles, centered on the Piton de la Fournaise volcano, sampled its eastern and southern flanks (Figure 2). They were recorded by eight OBSs (numbered 2 to 9) as well as by up to 55 LS deployed on the active volcano itself. A 250 km long profile was shot between Mauritius Island and La Réunion and southwest of La Réunion along the presumed track of the hotspot [*Gallart et al.*,

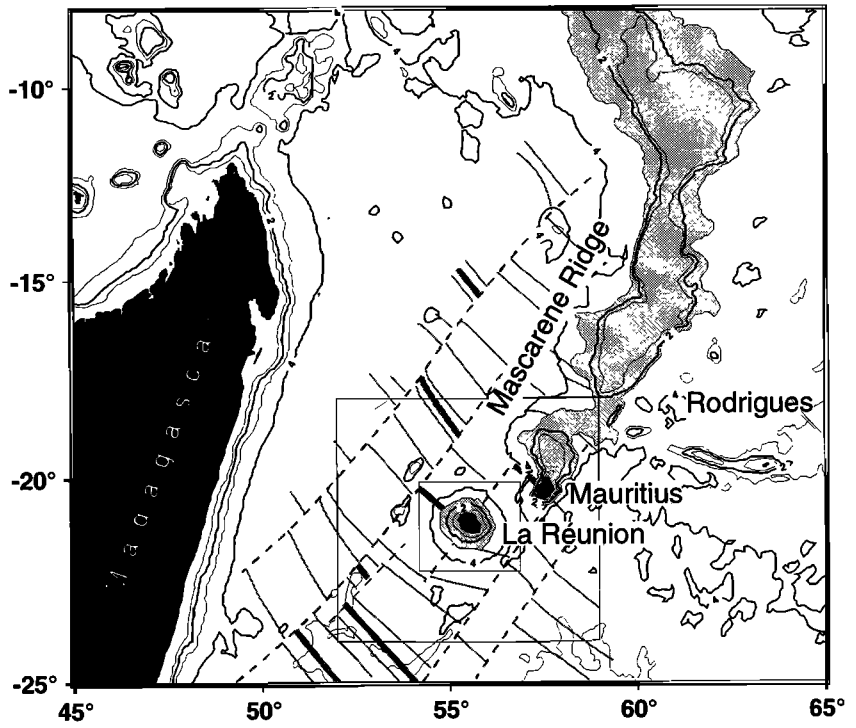

Figure 1. General location of La Réunion, Mauritius, and Rodrigues islands and of the Mascarene Ridge (shaded area) related to hotspot activity. Magnetic anomalies are shown as thin shaded lines, fracture zone as thin dashed lines, and extinct spreading centers as thick shaded lines [after *Dyment*, 1991]. The large box is the area used for the computation of gravity anomalies, the small box corresponds to the study area shown in Figures 2 and 14.

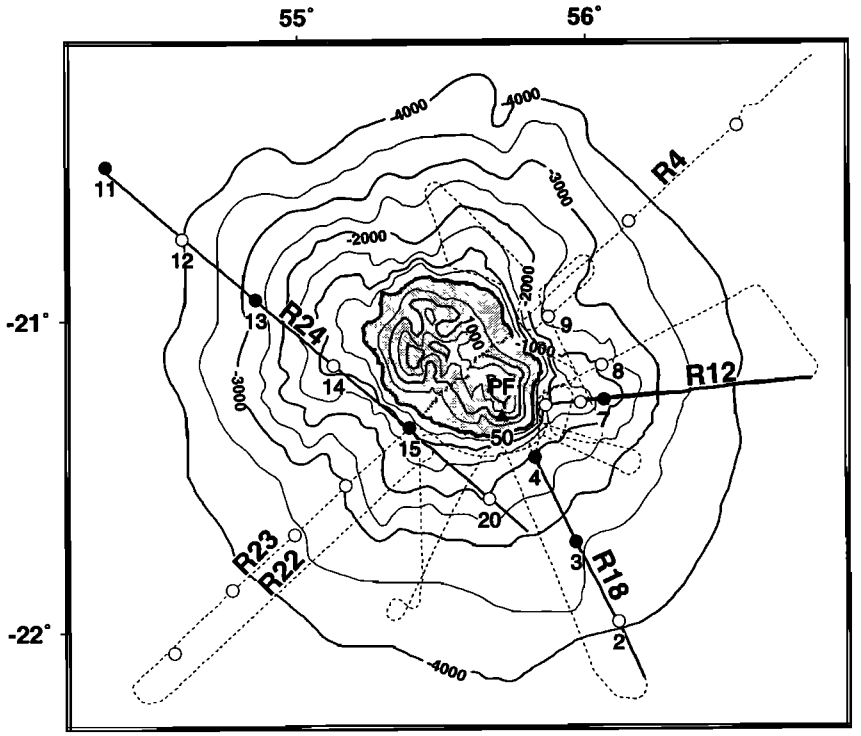

Figure 2. Location of the seismic profiles shot during the RÉUSIS (Réunion Sismique) experiment. Wide-angle seismic profiles discussed in this paper are drawn with solid lines, whereas other seismic profiles are dashed. Ocean bottom seismometer (OBS) locations are indicated by solid circles when the corresponding record section is shown and by open circles otherwise. Locations of land station (LS) 50 used along line R18 is indicated by a solid triangle. Line and OBS labels used in the text are also indicated. Bathymetry is from *Lénat and Labazuy* [1990].

this issue]. Profile R24 was shot perpendicular to the track of the hotspot over six OBSs (numbered 11 to 15 and 20, Figure 2).

The seismic source consisted of an untuned array of eight air guns, 16 L each, fired simultaneously every 80 s (200 m spacing) at a pressure of 140 bars. The receivers were three-component digital (4.5 Hz geophones) OBSs recording the seismic signal continuously at 10-ms sample interval with an antialias low-pass filter at 30 Hz [*Nakamura and Garmany*, 1991]. The exact locations of the OBSs on the bottom were computed using a least squares inversion of water wave travel times [*Nakamura et al.*, 1987]. A Global Positioning System (GPS) clock was used as the on-board reference to correct OBS clocks and to provide shot timing. The ship's location was recorded for each shot using the civilian channel of the GPS.

The seismic signal is band limited to 5-15 Hz with a dominant frequency of 9 Hz. To attenuate noise observed on record sections of OBSs deployed in shallow water, seismograms were band-pass filtered using a minimum phase Butterworth filter between 3 and 12 Hz for travel time picking. We used a spectral minimum phase deconvolution (whitening) to decrease source effect and to ensure accurate picking of travel times.

The data were modeled using a two-dimensional (2-D) iterative, damped, least squares inversion of travel times [*Zelt and Smith*, 1992]. We obtained the gross two-dimensional velocity model of the structure using travel time inversion and a layer-stripping approach, proceeding from top to bottom of the structure. Travel time inversion was further constrained with amplitude modeling, using asymptotic ray theory synthetic seismograms, in order to estimate vertical gradients in the layers.

We checked for consistency between the results inferred from the interpretation of MCS data and the model derived from wide-angle seismic data only by converting the velocity model into reflection times. The computed two-way travel times for the main interfaces, top of the oceanic basement and base of the crust, are consistent with the times observed on the MCS sections where the corresponding interfaces are distinct. Refraction allows us to extend the model near the island, where the MCS data are plagued by multiples and side echoes.

However, a systematic discrepancy is outlined between the top of the low-velocity layer interpreted as preexisting oceanic sediments from the MCS data [*de Voogd et al.*, this issue] and the top of the layer associated with the shadow zone observed on wide-angle seismic data recorded close to the island. In the final model, the shadow zone constrained by amplitude modeling of wide-angle seismic data incorporates a low-velocity layer whose top is constrained by the MCS travel times, as discussed in section 3.3. Hence a model can be found that is consistent with the results of both seismic methods, but each of them taken alone would have emphasized a different aspect of the structure.

3. Topography of the Oceanic Basement and Seismic Velocities in the Volcanic Edifice

The MCS data presented by *de Voogd et al.* [this issue] suggest that the top of the preexisting oceanic plate is not systematically dipping toward La Réunion as is the case in a Hawaiian-type island [*Watts et al.*, 1985; *Wessel*, 1993]. Along profile R23, on the southwestern flank, the oceanic basement deepens towards the island whereas along profile R4 on the northeastern flank, it gets shallower [*Gallart et al.*, this issue]. In this part of our study we analyze the topography of the oceanic basement along the different wide-angle seismic lines available (Figure 2).

3.1. Basement Step Across an Inferred Fracture Zone: Profile R24 (OBS 15)

On the split-spread record section of the WNW-ESE line located south of the island obtained by OBS 15, the southeastern branch of seismic phase 3, refracted in the oceanic crust, is 1.0 s late compared to the northwestern branch, suggesting that the top of the oceanic basement is deeper southeast of OBS 15 (Figure 3). From the geometry of the profile, this change in the depth of the oceanic basement can be constrained to occur within 15 km of OBS 15. MCS lines R22 and R23 [*de Voogd et al.*, this issue] show that the oceanic basement is deeper southward (i.e., on profile R22). This change in the depth of the oceanic basement is imaged at the far offshore end of profiles R22 and R23, as a steep scarp which reaches 0.5 km, assuming a velocity of 3.3 km/s in the oceanic sediments [*de Voogd et al.*, this issue]. This tectonic feature, parallel to and located between profiles R22 and R23, is interpreted as a transform fault of the preexisting oceanic crust and coincides with an offset in magnetic lineations [*Dyment,*

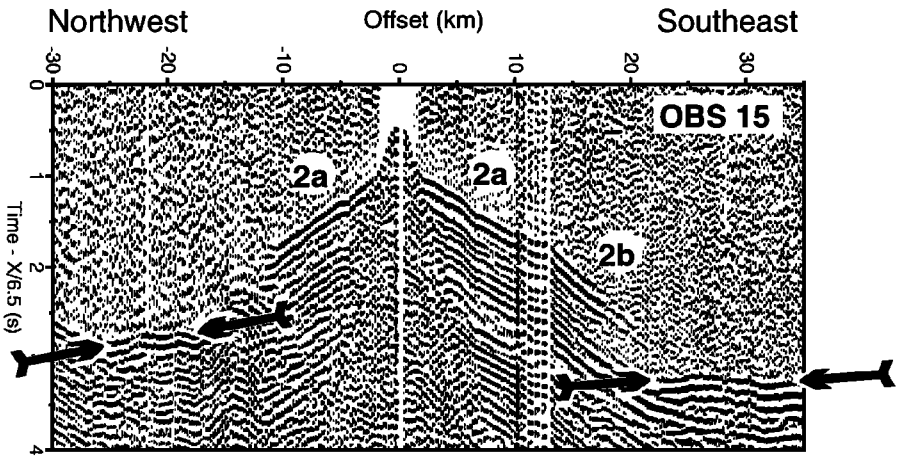

Figure 3. OBS 15 record section along profile R24. Reduction velocity is 6.5 km/s. The seismic section is corrected for bathymetry. Arrival of the wave refracted in the oceanic crust (arrows) are ~1 s later on the southeastern side of OBS 15. This delay suggests that the oceanic basement is deeper southeast of OBS 15.

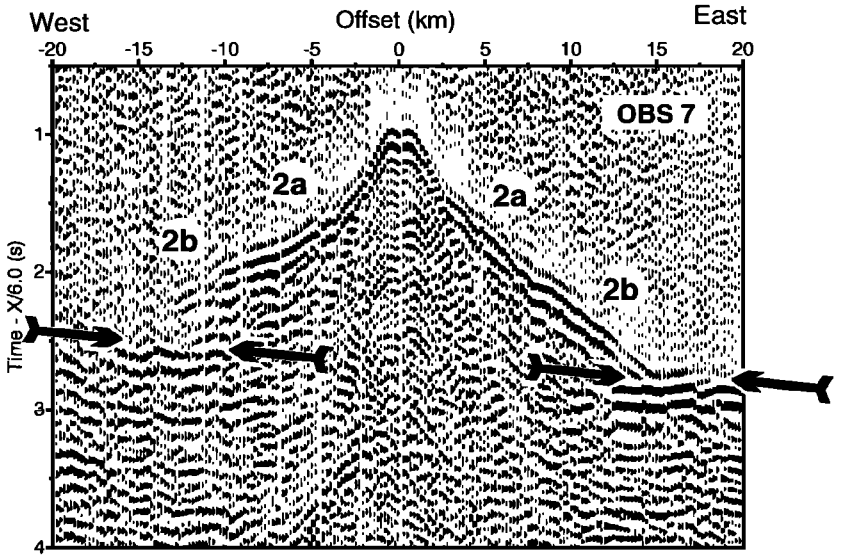

Figure 4. OBS 7 record section along profile R12. Reduction velocity is 6.0 km/s. The seismic section is corrected for bathymetry. The arrival refracted in the upper oceanic crust, indicated by arrows, illustrates that the top of the oceanic crust is dipping eastward, away from the island, along this profile.

1991]. Split-spread profile R24 recorded on OBS 15 allows us to determine the velocity in the volcanic and sedimentary pile (3.6-4.3 km/s); hence there is a vertical offset of the oceanic basement near the island, where the MCS data are obscured by multiples.

3.2. Rise of the Basement Toward the Island Beneath the Eastern and Southern Flanks of Piton de la Fournaise: Profiles R12 on OBS 7 and R18 on OBS 4

Beneath the eastern flank of the edifice, along line R12, the OBS 7 record section (Figure 4) shows phases labeled 2a and 2b interpreted as refractions in the volcanic pile of the Réunion edifice, with apparent velocities of 3.0 and 3.5 km/s, respectively. A phase observed on both sides of the OBS between 10 and 20 km offset (Figure 4), with a higher apparent velocity on the western side of the OBS, is interpreted as a refraction in the upper part of the oceanic crust. The increase of the reduced travel times of this phase to the east implies that the oceanic basement is dipping away from the island if we assume no lateral variation of the average velocity in the overlying volcanic and sedimentary pile. Assuming a constant dip for the interfaces and a constant velocity in each layer, the split-spread profile R12 constrains both the velocity in the underlying oceanic crust and the true depth to the oce-

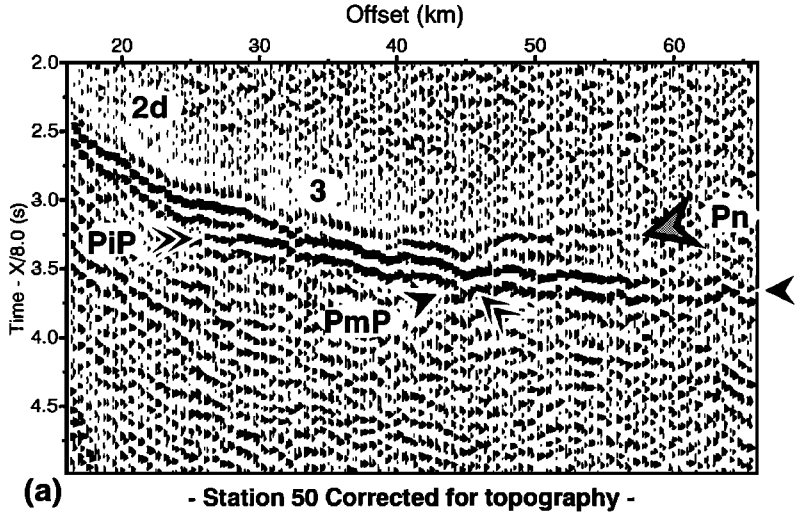

Figure 5. (a) Record section from station 50 (line R18) showing evidence for crustal underplating. The section is corrected for topography and has a reduction velocity of 8.0 km/s. Data are whitened and band-pass filtered at 5-12 Hz using a minimum phase Butterworth filter. An automatic gain control (1 s window) is used to enhance low amplitude arrivals. Solid arrows indicate reflection from the base of the crust (*PmP*), the shaded arrow indicates the refraction from the upper mantle (*Pn*) and the double arrows indicate a deep reflection (*PiP*) that we interpret as the reflection from the top of the underplated body. (b) Same as Figure 5a, but for record section from OBS 4. The white arrow indicates the intersection between the refraction traveling in the crust and the reflection from the Moho. (c) same as Figure 5a, but for OBS 3.

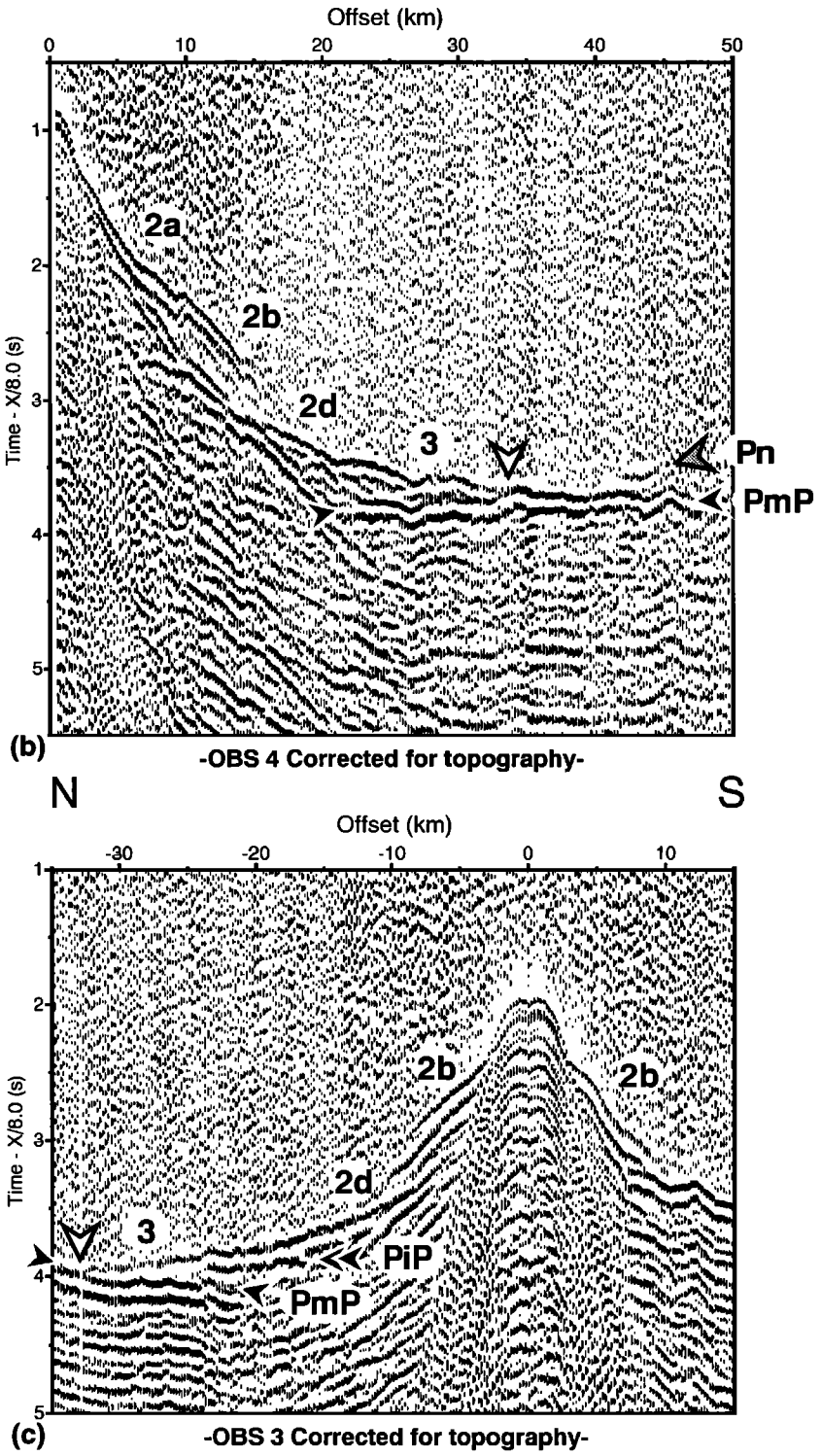

Figure 5. (continued)

anic basement. The dip of the oceanic basement is ~4°, and its depth is ~6 km, beneath the OBS. The average velocity in the upper oceanic crust is ~6 km/s. The existence of a clear shadow zone west of the OBS, at ~13 km offset and its absence to the east, suggests that the average velocity in the volcanic pile may increase eastward. This would imply an even larger dip of the oceanic basement away from the island. Similarly, line R18 to the southeast, recorded by land station 50 and OBS 4 (Figures 5a and 5b), again provides evidence for a dip of the oceanic basement away from the island if we assume there is no lateral variation of the velocity in the upper oceanic crust. The basement is at a depth of ~4 km beneath the western end of profile R12 and at the northern end of profile R18, substantially shallower than the oceanic basement farther away from the island whose average depth is ~5 km. With the velocity control provided by refraction data, this confirms the image of a rise of the oceanic basement toward the island inferred from the analysis of MCS profiles in this area [*de Voogd et al.*, this issue].

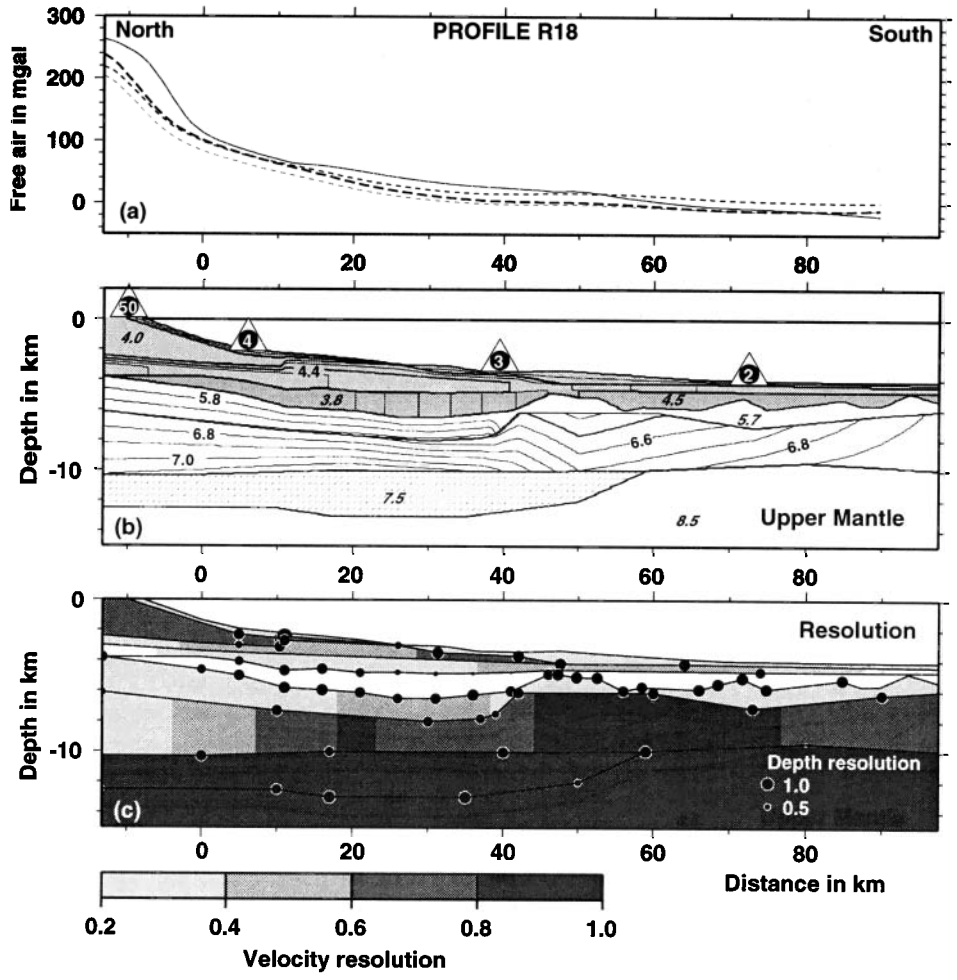

Figure 6. (a) Comparison between the observed gravity anomalies (solid line) along line R18 (Figure 14) and gravity anomalies computed in a 3-D model derived from seismic interpretation as described in Table 1. Gravity anomalies are computed for three different values of the density of the volcanic edifice: 2500 kg/m^3 (light dashed line), 2600 kg/m^3 (medium dashed line), 2700 kg/m^3 (bold dashed line). (b) Model obtained from travel time inversion and amplitude modeling along line R18. Vertical exaggeration is 2. Isovelocity contours are drawn at 0.1 km/s with annotations. Interval velocities are italicized. The boundaries between the main crustal layers are underlined by thick lines. Locations and labels of OBS and LS are indicated along the profile. The volcanic edifice is outlined with light gray whereas the preexisting oceanic sedimentary layer inferred from MCS data is darker. The underplated layer is outlined by a discontinuous hachured pattern. The root mean square (RMS) between observed and computed travel times is 0.06 s for wide angle travel times and 0.08 s for normal incidence travel times. (c) Resolution of the parameters of the model as defined by *Zelt and Smith* [1992]. Resolution of velocities computed with a fixed velocity gradient is shown by a gray scale in layers. Resolution of the depth nodes defining interfaces between layers is indicated by dots scaled proportionally to the resolution value. The high resolution (>0.8) computed in the underplate and in the upper mantle is because we assume a constant velocity in these layers.

3.3. Edifice Stratification From the Velocity-Depth Function Beneath the Southeastern Flank of Piton de la Fournaise: Profile R18

Phase 2b, refracted in the Réunion volcanic edifice, disappears abruptly at ~15 km on the OBS 4 record section and more progressively, with an en echelon pattern, at ~10 km north of OBS 3 (Figure 5). This shadow zone exists neither to the south of OBS 3 nor on the OBS 2 record section farther offshore. It can be related to a low-velocity layer located between the volcanic pile and the oceanic basement or to a layer with no vertical velocity gradient. The existence of a low-velocity layer at the base of the volcanic edifice has also been inferred from velocity analysis of MCS data and from the polarity of signals reflected from the top of this layer. This reflector is interpreted as the bottom of the volcanic construction on top of the oceanic sediments [*de Voogd et al.*, this issue]. We assume the features observed on the wide-angle and multichannel seismic data are related to a single low-velocity layer. Reflection two-way times for the top of the low-velocity layer, picked on the MCS profiles, are hence introduced in the ray-tracing modeling to constrain the top of the low-velocity layer (dark gray layer, Figure 6b). Such a model cannot account for the observed amplitude since the decrease of the amplitude would occur in the wide-angle synthetic seismograms at distance greater than observed (Figure 7). Since the distance at which the amplitude of the phase refracted in the overlying layer decreases is

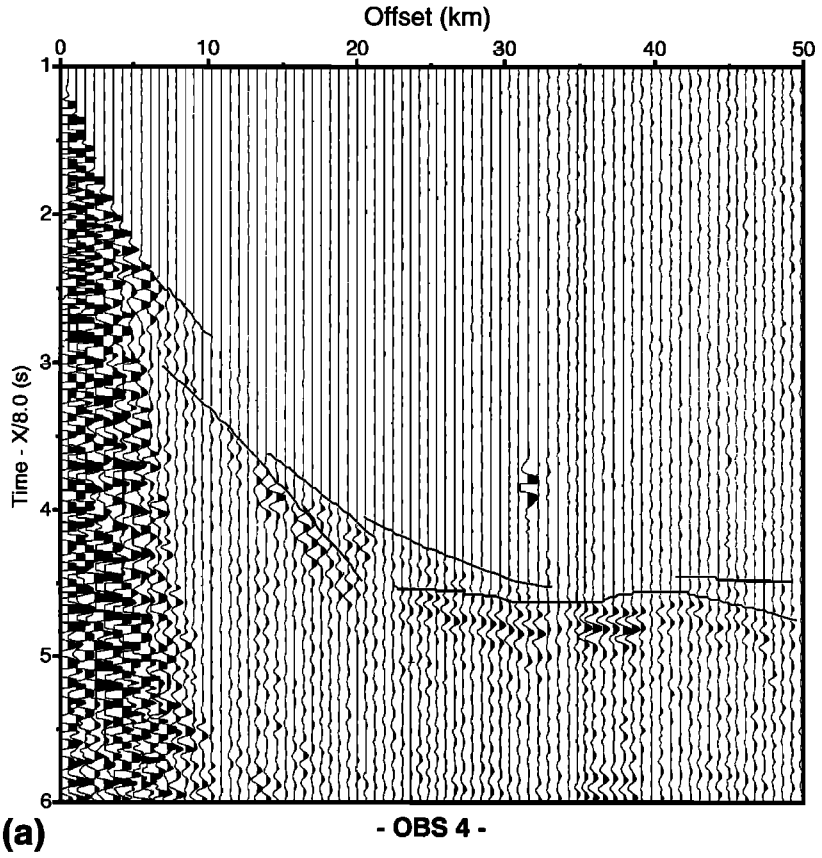

Figure 7. Amplitude modeling for OBS 4 (line R18). (a) Data are presented with an amplitude scaled proportionally to squared distance (one trace out of three is shown, resulting in interval of ~600 m between traces). Thin lines are travel times within the final velocity model (Figure 6) for the main arrivals observed on the seismic section. (b) Synthetic seismograms, computed in the final velocity model (Figure 6), plotted at 600 m intervals with an amplitude scaled proportionally to distance. Thins lines are computed travel times to help in comparing with the data. (c) Synthetic seismograms computed in a 2-D velocity model identical to the final model presented in Figure 6 except for the layer immediately above the low-velocity layer where the velocity increases steadily with a vertical gradient of 0.2 s^{-1} (solid curve in the inset). The wave refracted in the volcanic pile vanishes abruptly at 18 km (open arrow), whereas this occurs at ~10 km on the data. The inset shows velocity versus depth functions beneath OBS 4 in the final velocity model (dashed line) and in a model without a second-order discontinuity in the volcanic pile (solid line). V indicates the base of the volcanic edifice, and B indicates the oceanic basement inferred from MCS travel times.

controlled by the vertical velocity gradient in the overlying layer and by the depth to the top of the low-velocity layer, the fit may be improved by changes in the overlying layer. In the final velocity model we add a layer with no vertical velocity gradient immediately above the low-velocity layer deduced from MCS in order to fit the observed amplitude on the OBSs (Figures 7 and 6). This layer, which is characterized by a constant velocity but with a rather high value of ~4.5 km/s with respect to the overburden, thins out south of OBS 3 (at ~40 km, Figure 6), as is suggested by the lack of shadow zone south of OBS 3 and on the OBS 2 record section.

The velocity in the low-velocity layer, presumably of oceanic sediments (3.8 km/s), is poorly constrained, but it is consistent with travel time modeling of both multichannel and wide-angle seismic data and with the amplitude of the phase reflected from the oceanic basement which appears clearly on OBS 4 record section between 8 and 20 km (Figure 7).

4. Topography of the Moho and Extent of the Crust-Mantle Intermediate Layer

The onshore-offshore transect presented by *Gallart et al.* [this issue] provides strong evidence for the existence of a layer of intermediate velocity at the base of the crust which we interpret as an underplated body. We now check for evidence for such a structure along other wide-angle seismic lines to determine the lateral extent of the body. We describe different types of seismic observations which can be interpreted as due to the presence of an intermediate velocity layer at the base of the crust.

4.1. Extent of the Crust-Mantle Intermediate Body Radially to the Southeastern Flank of Piton de la Fournaise: Profile R18

One or two phases, reflected from near the base of the crust are clearly visible on the LS 50, OBS 3, and OBS 4 record sections

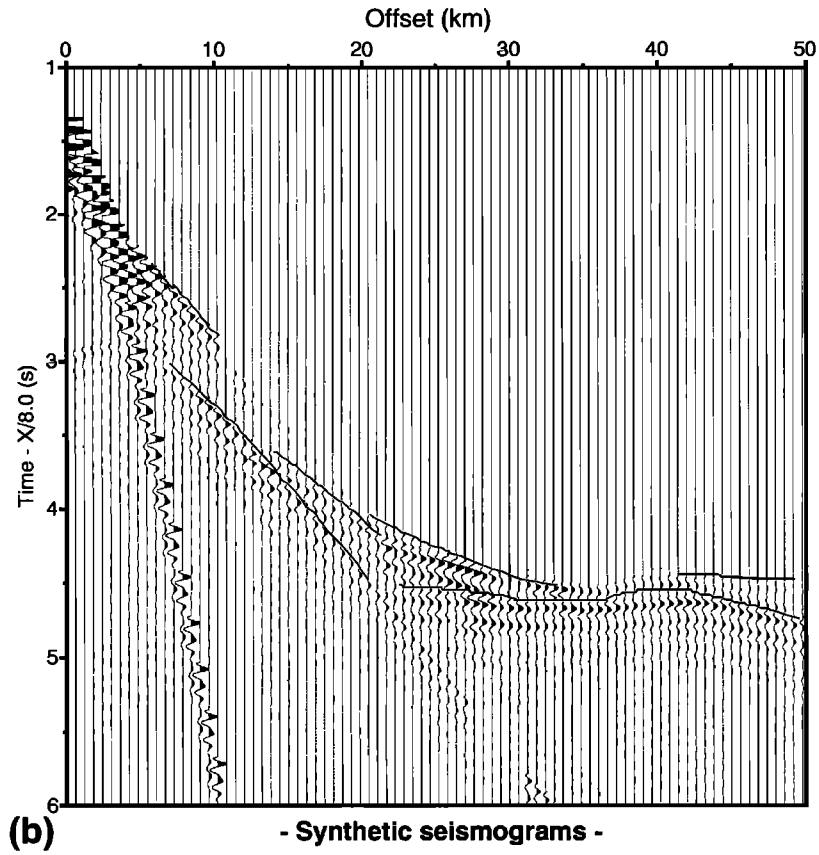

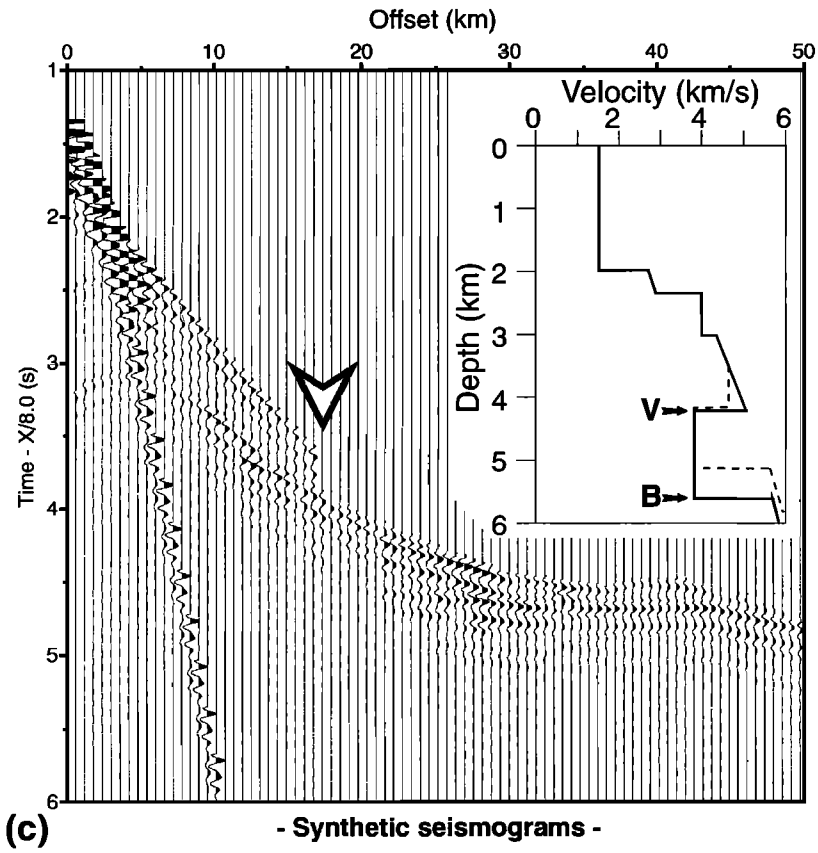

Figure 7. (continued)

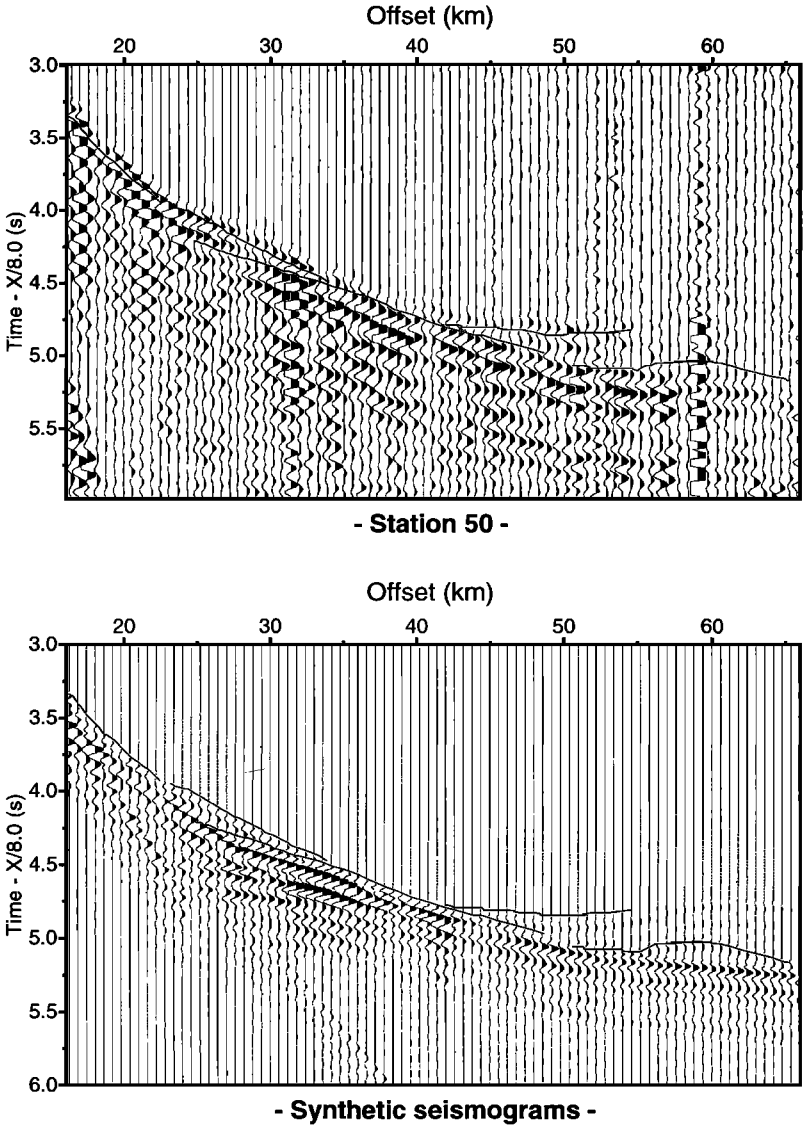

Figure 8. Amplitude modeling for station 50 (line R 18). Same as Figure 7.

(Figure 5). The *Pn* wave, refracted in the upper mantle, is only identifiable on the LS 50 and OBS 4 record sections with an apparent velocity of ~8.4 km/s. The emergence of the *Pn* arrival from one of the reflected phases allows us to interpret this phase as *PmP*, the Moho reflection, with a critical distance at ~34 km (Figure 5).

The position of phase 3, refracted in the lower crust, relative to *PmP* is uncommon, since the postcritical *PmP* has an apparent velocity faster than phase 3 (Figure 5). In a simple model of the crust-mantle transition where the lower crust directly overlies the upper mantle, the travel time curves of phase 3 and *PmP* would be asymptotic at far range. The phase geometry suggests that the velocity above the mantle, inferred from postcritical travel times of *PmP*, is higher than the velocity in the lower crust defined from the travel time of phase 3. In other words, we have to introduce an intermediate layer, located between the lower crust and the upper mantle, in order to account for this observation (Figure 6). On LS 50 and OBS 3 record sections, a second arrival (double arrow, Figure 5a) can be interpreted as a reflection from the top of the intermediate layer (*PiP*). These are the only record sections where *PiP*, reflected from the top of the intermediate layer, and *PmP*, reflected from the top of the upper mantle, are both visible. The velocity in the intermediate layer (~7.5 km/s) is controlled by the postcritical travel time of *PmP* and also by the relative amplitude of *PmP* and *PiP* that constrains the velocity contrast at the top and at the bottom of the layer (Figures 7 and 8). The velocity in the upper mantle is inferred from the unreversed *Pn* observed on LS 50 and OBS 4 record sections. Owing to the scarcity of information, we assume a constant velocity (with no lateral or vertical gradient) in the intermediate layer and in the upper mantle as well (Figure 6). The geometry of the top of the intermediate layer and of the top of the upper mantle is defined by travel times of phases *PiP* and *PmP*.

The thickness of the preexisting oceanic crust (in the area where the resolution is greater than 0.4, Figure 6) ranges between 4 and 6 km which is slightly lower than the mean crustal thickness for normal oceanic crust (7.08 ± 0.78 km [*White et al.*, 1992]). This may be related to the closeness of fracture zones [*Dyment*,

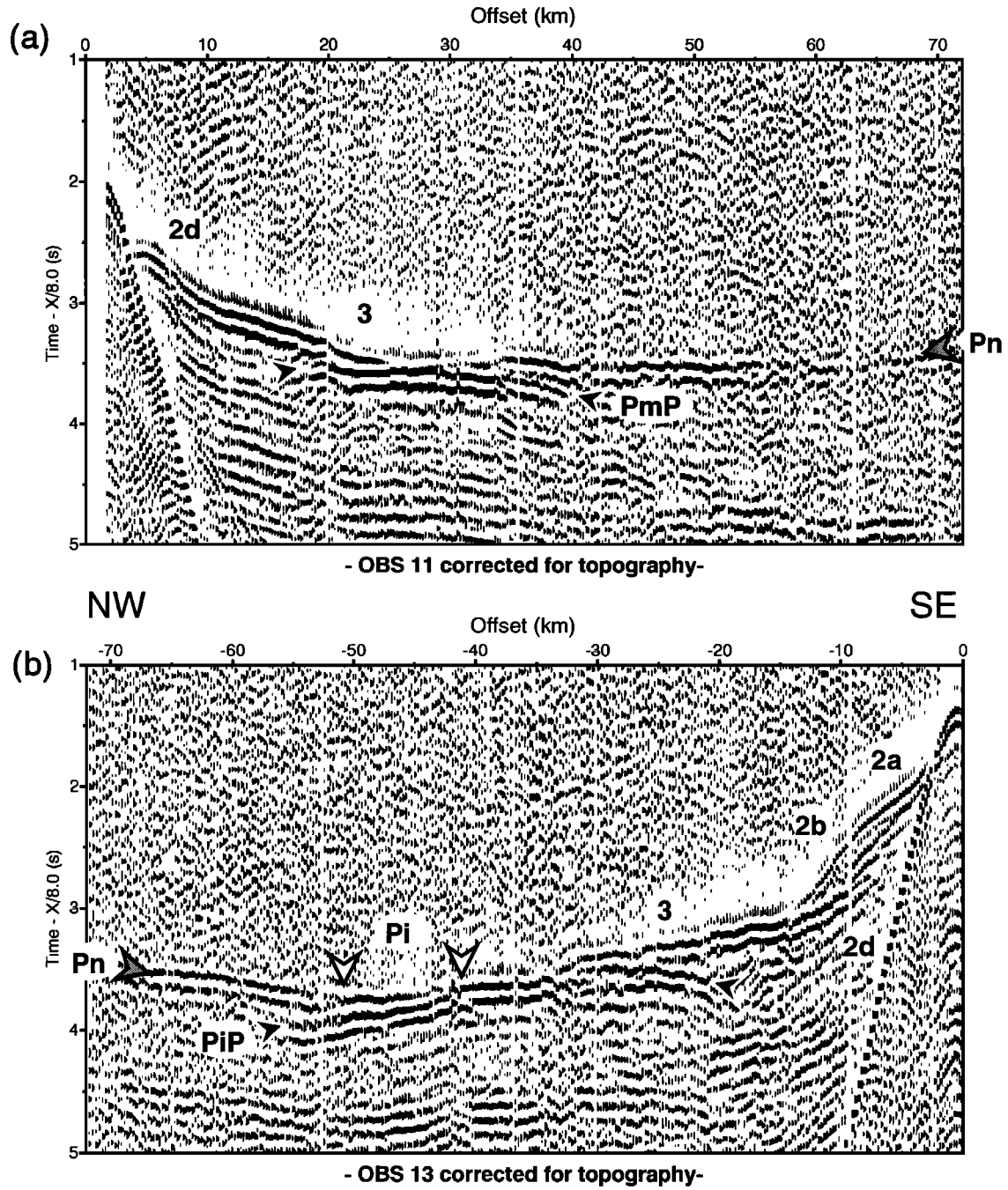

Figure 9. (a) OBS 11 and (b) 13 record sections along profile R24 showing the edge of crustal underplating. Same as Figure 5.

1991] where the crust is generally thinner than normal oceanic crust (4.0±1.3 km [*White et al.*, 1992]). Velocities in layers 2 and 3 range between 5.7-6.0 and 6.5-7.1 km/s respectively, with a similar vertical velocity gradient (0.10-0.15 s^{-1}). They are in the range of velocities described in typical oceanic crust [*White et al.*, 1992].

4.2. Extent of the Intermediate Body Across the Hotspot Track: Line R24

The seismic section recorded by OBS 11, located at the northwestern end of line R24 (Figure 2), appears as a typical oceanic section. There is no visible arrival refracted in the sedimentary cover. Two phases refracted within the igneous crust (labeled 2d and 3, Figure 9a) are observed as first arrivals. The *PmP* phase is observed between 18 and 40 km; its critical distance is located at ~27 km, and *Pn* has an apparent velocity of 8.0 km/s. The relationship between phase 3 (refracted in the lower oceanic crust) and *PmP* is classical for a simple Moho interface, these two phases merging around 27 km of distance.

The record section from OBS 13, located at ~40 km from the island, also exhibits a typical relation between phase 3 refracted in the lower oceanic crust and the reflection labeled *PiP* (Figure 9b). The apparent velocity of phase 3 is similar to the postcritical velocity of the deep reflection *PiP* (Figure 9b, to compare with OBS 4 and 3 record sections, Figure 5). These two arrivals merge at

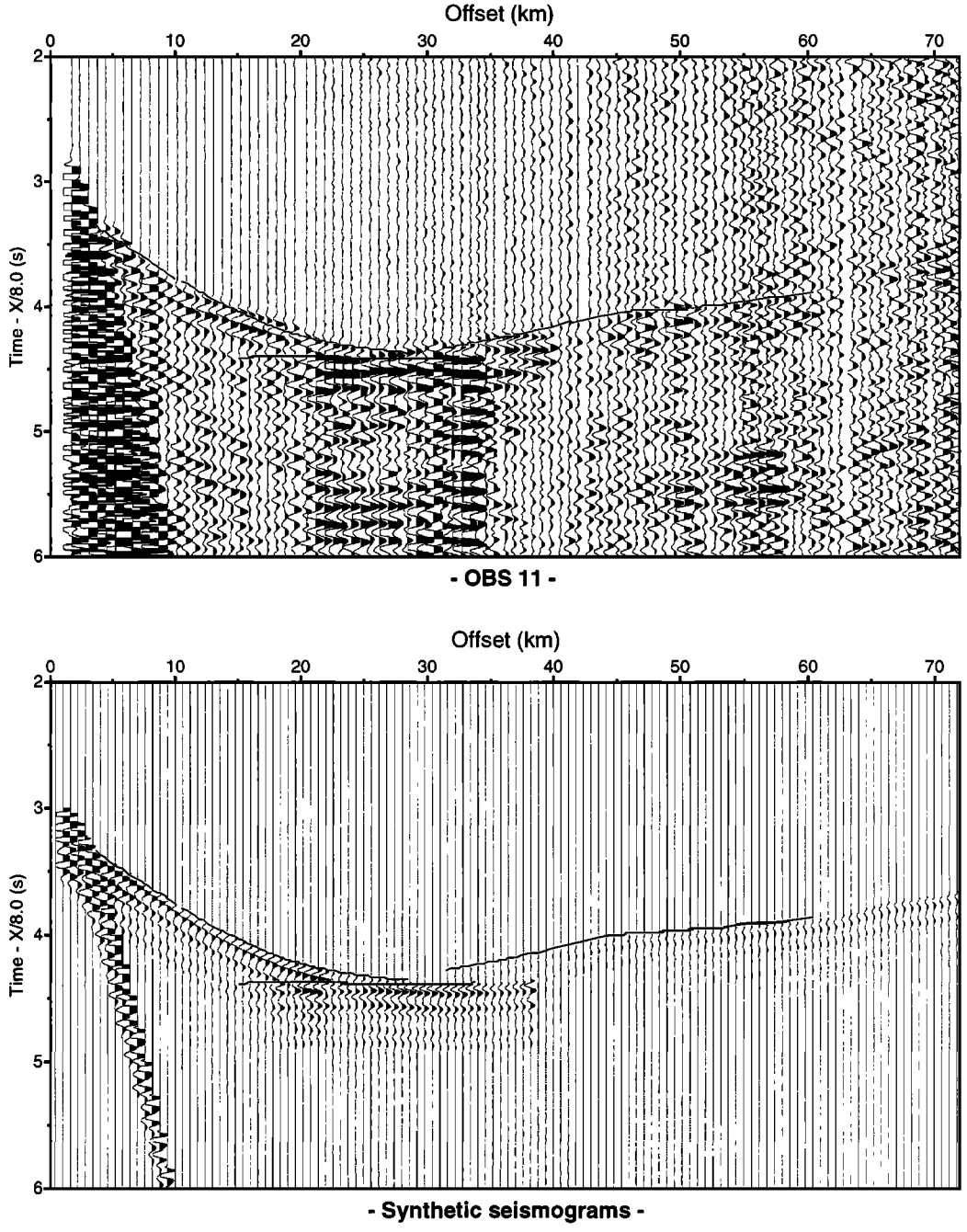

Figure 10. Amplitude modeling for OBS 11 (line R24). Same as Figure 7.

~40 km and cannot be separated at larger distances. This geometry proves that the energy reflects from the base of the crust. At 42 km range, a refraction with an apparent velocity (corrected for topography) of ~7.8 km/s emerges as first arrival. Beyond 50 km range, the first arrival exhibits an apparent velocity (corrected for topography) as high as 8.9 km/s that can only be due to refractions in the upper mantle. This feature is very similar to the feature observed on stations 7 and 35 along line R23 [*Gallart et al.*, this issue, Figure 4]. The arrival observed between 42 and 50 km is interpreted as a refraction in an intermediate layer located between the lower crust and the upper mantle (*Pi*). The deep reflection visible on OBS 13 (*PiP*) is related to energy reflected from the top of the intermediate layer (i.e., the base of the lower crust). There is no evidence of energy reflected from the Moho on this section, but the contrast between the velocity in the intermediate layer and the upper mantle is small (0.2-0.3 km/s). There is similar evidence for an intermediate layer located at the base of the crust on the southeastern part of the OBS 12 record section, toward the island (Figure 2).

On the OBS 11 record section, phase 2d, refracted in the upper oceanic crust, exhibits a clear curvature with high amplitude which was modeled by a high-velocity gradient. The velocity increases from 5.2 km/s at the top to 6.6 km/s at the bottom of this layer, which we interpret as the oceanic layer 2 (Figures 10-12). There is no marked velocity discontinuity between layer 2 and layer 3, but there is a change in the vertical velocity gradient that

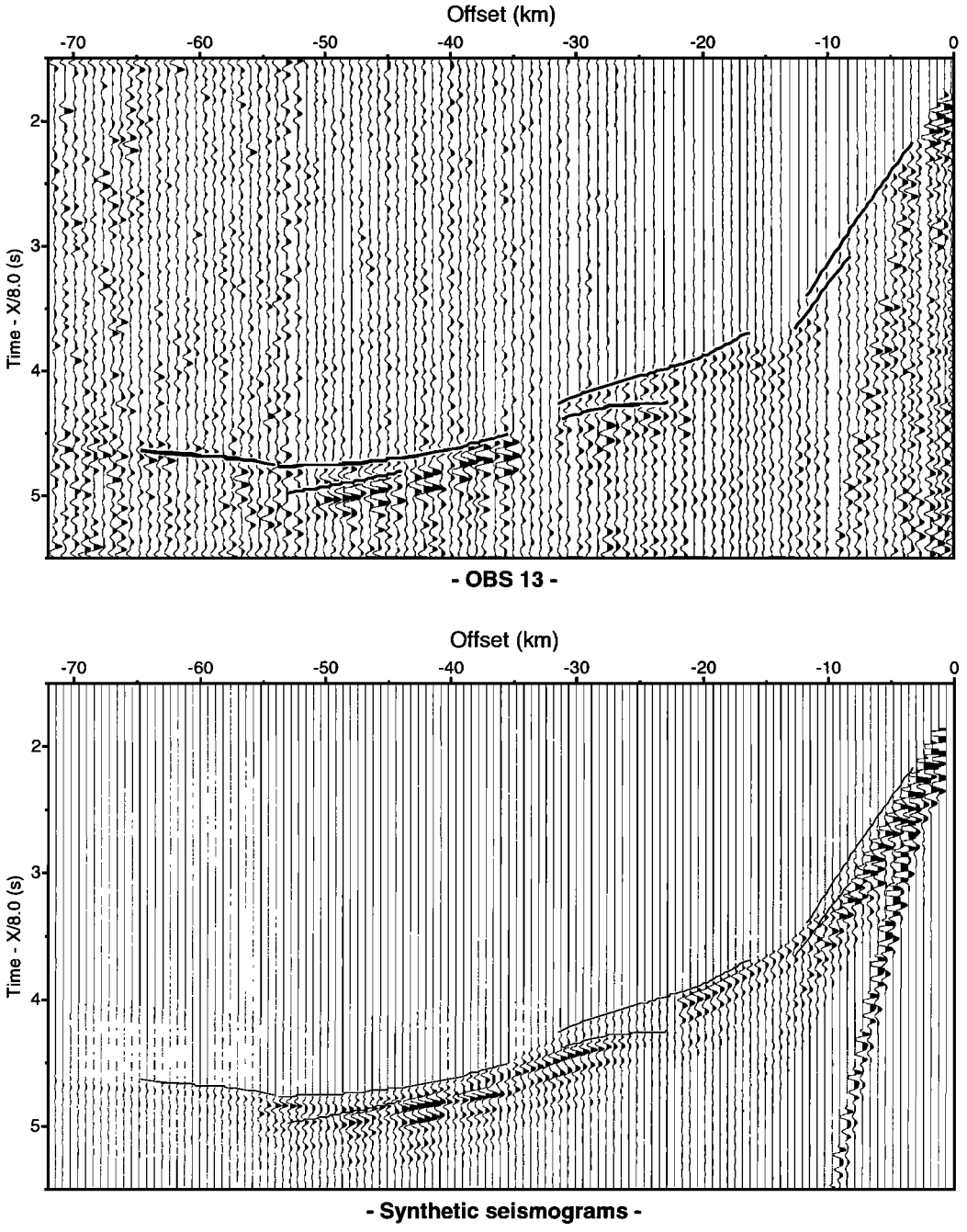

Figure 11. Amplitude modeling for OBS 13 (line R24). Same as Figure 7.

decreases from ~0.5 s^{-1} in layer 2 to ~0.15 s^{-1} in layer 3, which is a common feature in normal oceanic crust [*White et al.*, 1992].

The final model obtained from travel time inversion and amplitude modeling shows that the intermediate layer thins out northwestward at ~20 km and reaches a maximum thickness of ~3 km beneath OBS 14 (Figures 10-12). The velocity in the intermediate layer is constrained by the arrival *Pi* observed on OBS 3 (Figure 9) and also by the amplitude of *PiP* and the lack of *PmP* (Figure 11), which are compatible with velocity contrasts of 0.6 and 0.2-0.3 km/s at the top and at the bottom of the intermediate layer. The deeper part of the model is poorly constrained south of OBS 14 because of the relatively low signal-to-noise ratio of the data, but we take into account the perpendicular line R23 in the final velocity model (Figure 12).

5. Implications and Discussion

We discuss in this section the features described at different levels in the lithosphere beneath La Réunion and compare with different intraplate marine volcanoes: submerged seamounts (e.g., Jasper seamount [*Hammer et al.*, 1994; *Hildebrand et al.*, 1989]), active volcanic islands (e.g., Hawaii [*Zucca et al.*, 1982]), extinct volcanic islands (e.g., Marquesas [*Holbrook*, 1995] and Oahu [*Watts et al.*, 1985]).

5.1. Stratification of the Edifice

Seismic velocities in the volcanic edifice are fairly uniform on the different profiles over its submarine part, which suggests that it is formed by volcanic material which is homogeneous at the

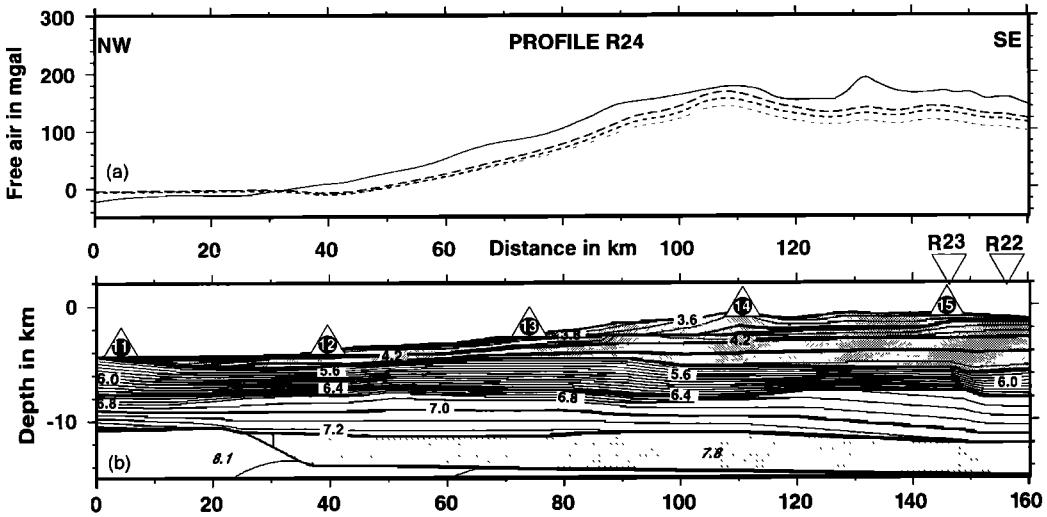

Figure 12. (a) Comparison between the observed gravity anomalies along line R24 (Figure 14). Same as Figure 6a. (b) Model computed along profile R24 using travel time inversion for OBSs 11 to 15 and 20 and amplitude modeling for OBSs 11-13. Vertical exaggeration is 2. Same as Figure 9 except for the gray pattern that includes both the preexisting oceanic sediments and the volcanic construction as we have no MCS data to locate the base of the edifice.

scale of our investigation (a few hundred meters). Velocities range from ~3.4 km/s near the surface to ~4.5 km/s at the bottom of the edifice. This increase with depth may either be due to a change in composition or be a result of the effect of compaction caused by successive deposits of the same material. The latter case is consistent with the view that successive slumps and debris avalanches constructed the bulk of the submarine edifice, as suggested from MCS [*de Voogd et al.*, this issue].

The shadow zone observed on many seismic record sections (e.g., Figures 3, 4, and 7) brings a complementary view to the MCS data in the lower part of the edifice. MCS data image the base of the edifice as a reflector at the top of a low-velocity layer, which is interpreted as the oceanic sedimentary cover predating volcanic activity and sealed by the volcano. On the other hand, the shadow zone in the wide-angle seismic data documents a sharp decrease of the vertical velocity gradient, but this occurs in the volcanic pile ~1 km above the base of the edifice defined by MCS. The constant velocity layer forming the deeper part of the edifice may be regarded as a layer of volcanic origin, but which has a "high velocity" (4.5 km/s) compared to the upper part of the volcanic pile (Figures 6 and 7). It could then be interpreted as comprising a material which is different from that deposited on its top by slope instability from the subaerial part of the island. The 4.5 km/s value of the velocity for the deeper part of the edifice is comparable to that of the material forming seamounts, as illustrated for Jasper seamount, where it is attributed to a pile of extrusives [*Hildebrand et al.*, 1989]. In the case of seamount volcanism, the material is deposited on top of a preexisting plate like for La Réunion but without contribution of subaerial flows. By analogy, this deeper volcanic layer at La Réunion could correspond to the edifice built by submarine flows during the initial stages of volcanism before emersion of the island. The 2a superficial layer of the present edifice underwater (Figures 6 and 12) has a seismic velocity significantly lower than 4 km/s and is likely made of material erupted subaerially, then transported downslope, as evidenced from sea bottom studies [*Lénat et al.*, 1989]. Layer 2b underneath may be transitional between submarine and subaerial. Hence it is difficult to estimate the proportion of submarine erupted material because it may not entirely be confined in the layer without velocity gradient between the base of 2b and the base of the edifice.

5.2. Oceanic Crust: Variations of Its Top and Thickness

The interpretation of refractions in the oceanic crust from wide-angle seismic profiles confirms independently the inferences from the MCS lines on the present depth and topography of its top. East and south of the island (i.e., along lines R4, R12, and R18) the oceanic basement rises toward the island with an amplitude of ~1 km relative to the average depth to the oceanic basement [*de Voogd et al.*, this issue]. South of the island, profiles R23 [*Gallart et al.*, this issue] and R24 show that the oceanic basement is up to 1.2 km deeper near the island, beneath OBSs 14 and 15, than in the adjacent basins. Some local offsets (Figure 12) are probably related to preexisting transform faults. The inferred basement depths are consistent with the lows of the oceanic basement inferred from MCS seismic lines in the same area [see *de Voogd et al.*, this issue, plate 1]. This topography of the basement could either be inherited or be related to reactivation of preexisting oceanic faults or be the consequence of plate flexure. In the latter case, a downwarping of the oceanic basement under the load of the island larger than 1.5 km is precluded by the seismic data

The thickness of the oceanic crust away from and beneath the volcanic edifice is rather constant (5-6 km) with a typical subdivision in layers 2 and 3. Velocities in oceanic layer 2 and especially the vertical velocity gradient are different between profiles R18 and R24 (0.15 and 0.5 s^{-1}, respectively). This difference does not seem to be related to the vicinity of the island, and it is probably due to a preexisting feature dating back to the initial emplacement of the oceanic crust (line R24 is closer to the extinct spreading center inferred from magnetic anomalies, Figure 1). Our models suggest that the volcanic activity has little influence on the structure of the preexisting oceanic crust in the outer parts of the submarine edifice. There is, however, evidence for a possibly slightly thicker crust under the island itself, since basement doming is seen from MCS and OBSs 7 and 4 profiles discussed earlier,

while the base of the crust remains level or slightly deepens toward the island and to the NNE, as seen on the 2-D section of R18 and discussed in section 5.3. Independent evidence for this slightly thicker crust toward the eastern part of the island results from a 3-D tomographic study of the active Fournaise volcano edifice [*Lankar-Bénichou*, 1997], using an array of 50 land stations recording all the radial profiles around it (Figure 2). Unfortunately, near the shoreline, the MCS is plagued by multiples and side echoes, and the distributions of OBSs or land stations lack continuity across the coast; hence the resolution of structure is not fine enough to provide an image of this intracrustal thickening, which allows us to discuss its origin. However, the image of the stratification of oceanic sediments trapped under the edifice shows they are tilted seaward [*de Voogd et al.*, this issue]. We conclude that the bulge of the top of the preexisting plate toward the island is related to the emplacement of La Réunion and not to the topography of the preexisting oceanic basement. Hence the slight thickening of the crust toward the island can be regarded as one of the causes of the doming of its top, and this thickening is likely due to intrusion by hotspot magmatism.

5.3. Topography of the Moho

Away from the island, the crustal structure is consistent with a 6-7 km thick oceanic crust with velocities in the lower crust between 6.6 and 7.3 km/s. Magmatic material has been added on the top and at the base of it. Several kinds of evidence for the presence of a layer between the crust and mantle, characterized by seismic velocities ranging from 7.5 to 7.8 km/s, have been described in this paper and in the paper by *Gallart et al.* [this issue]. We interpret the top of the intermediate velocity layer, which is a prominent reflector at the base of a normal oceanic crust (*PiP*, Figures 5 and 9), as the prevolcanic Moho.

The results obtained from all the wide-angle seismic lines, including R4-R23 [*Gallart et al.*, this issue], were compiled to produce two isobath maps: one for the base of the preexisting oceanic crust and one for the present-day Moho or top of the normal velocity upper mantle (Figure 13). The depth to the base of the preexisting oceanic crust increases gently to the NNE from 10 to 12 km. Beneath the southwestern flank of the volcanic edifice, a small increase in depth to the base of the crust, <1 km with a circular shape (Figure 13), should be related to the edifice load. This interface is interpreted as the relict of the former base of the crust, and it is the best indicator of plate flexure if we assume that it was not affected by magmatism. The depth to the top of the normal velocity mantle, or present-day Moho, located at the base of the underplated body (Figure 13), increases by up to 2 km with a maximum southwest of the island. This increase is mainly related to the thickening of the intermediate crust-mantle velocity body which reaches its maximum thickness (~3 km) at 25 km southwest of the island (Figure 13). There is no evidence of crustal underplating beneath the northeastern flank of the island, nor between Mauritius Island and La Réunion along the track of the hotspot. The intermediate body is elongated perpendicularly to the presumed hotspot track and centered ~25 km southwest of the island.

Using the relict prevolcanic base of the crust as a marker leads to a similar conclusion as the use of the oceanic basement or the use of the base of the edifice from MCS [*de Voogd et al.*, this issue]: there is no flexure of the lithosphere, resulting from the load of volcanic products, larger than 1.5 km. This result is very different from previous estimates based on modeling of geoid and gravity data that led to values of the maximum deflection as large as 4 to 5 km [*Bonneville et al.*, 1988; *Malengreau*, 1995]. Next we check if our seismic model is compatible with the observed gravity anomalies.

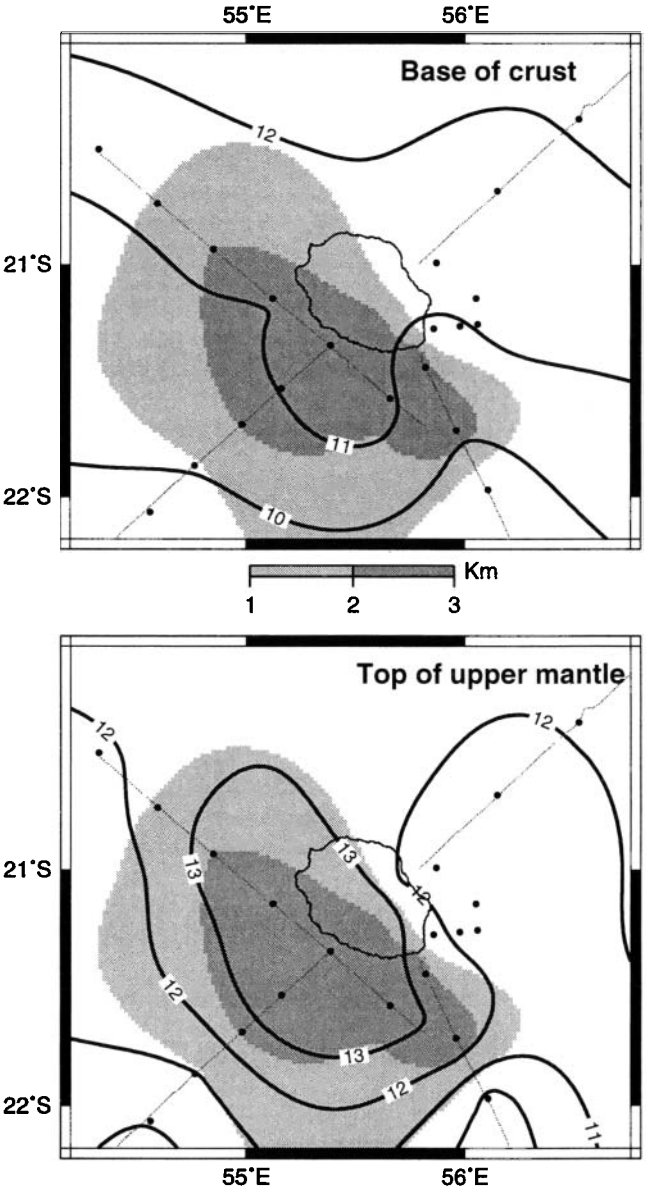

Figure 13. Maps that result from the compilation of depths modeled along all the wide-angle seismic lines shot during the RÉUSIS experiment (this paper and *Gallart et al.* [this issue]). The thickness of the underplated body is indicated in gray: <1 km, not relevant; between 1 and 2 km thick, light shading; >2 km, dark shading. Locations of OBS and shooting lines are indicated. (top) Topography of the original Moho (top of the underplated body) in km. (bottom) Topography of the present Moho (top of the "normal" upper mantle at the base of the underplated crustal body).

5.4. Gravity Implications

The regional gravity map is obtained, at sea, from a compilation of available ship-borne gravity data and satellite derived free air anomalies [*Sandwell and Smith*, 1997], and on the island, from the published Bouguer gravity anomalies [*Malengreau*, 1995; *Rousset et al.*, 1987]. Bouguer anomalies clearly depend on the density assumed for the Bouguer and terrain corrections; however,

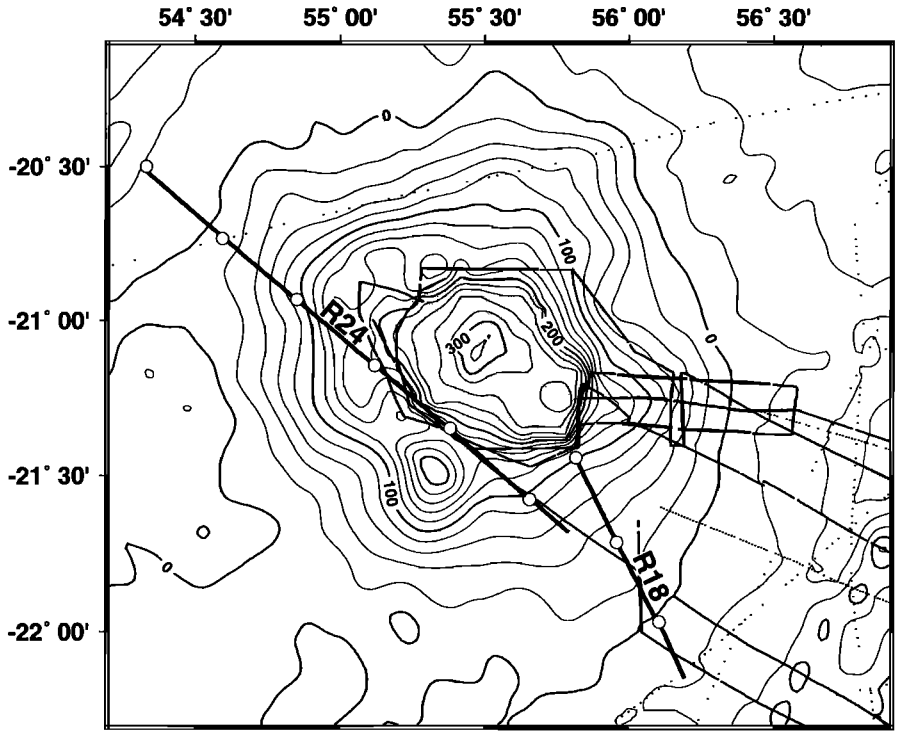

Figure 14. Gridded gravity anomalies around La Réunion using free air anomalies at sea and Bouguer anomalies (computed with a density of 2.67) on land. Free air satellite-derived data were used for areas more than 10 km away from a ship track. Dots mark gravity measurements at sea used in this map. The ship-borne data were shifted prior to combination by -10 mgGal. Seismic lines R18 and R24 are shown with the location of deployed OBSs (open circles). La Réunion is shaded.

these data contribute rather little to our modeling of offshore profiles. The different data sets were merged and gridded as described by *Minshull and Brozena* [1997] and displayed in Figure 14.

The gravity response of the 3-D seismic model was computed using the Fourier method of *Parker* [1974] for an area large enough to avoid edge effects in the vicinity of the island (Figure 1 and Table 1). We use a density of 2800 kg/m^3 for the oceanic crust, 3300 kg/m^3 for the mantle, and 2300 km/m^3 for the compacted sediments beneath the volcanic load. The average velocity in the volcanic edifice, calculated along the line R4-R23 [*Gallart et al.*, this issue] is ~4.2 km/s, including the high-velocity body located beneath the central part of the island. This is significantly lower than that of the oceanic crust, and we assign this layer a reduced density of 2500-2700 kg/m^3. The likely density of the underplate depends on whether its reduced velocity is due to partial melt or to mafic intrusions, but the resulting gravity anomaly is rather insensitive to the density used since the underplate is not very thick; we use a value of 3000 kg/m^3, intermediate between crust and mantle values.

The computed anomalies are shifted by a constant so that the mean misfit between the computed and the observed anomalies is

Table 1. Description of the Model Used for Gravity Anomalies Computation

	Description of Interfaces	Reference	Extrapolation	Density Contrast Across Interface, 10^3 kg m^{-3}		
				2500	2600	2700
1	bathymetry	[*IOC et al.*, 1997]	no	1.5	1.6	1.7
2	base of the volcanic edifice	*de Voogd et al.* [this issue] and *Gallart et al.* [this issue]	bathymetry	-0.2	-0.3	-0.4
3	top of oceanic crust	*de Voogd et al.* [this issue] and *Gallart et al.* [this issue]	1 km beneath bathymetry		0.5	
4	base of oceanic crust	*Gallart et al.* [this issue] and this study	12 km depth		0.2	
5	top of upper mantle	*Gallart et al.* [this issue] and this study	12 km depth		0.3	

The interfaces are defined by seismic data (except for bathymetry) available around La Réunion and extrapolated to a larger area, between 24°S and 18°S latitude and 52°E and 59°E longitude, to avoid edge effects (Figure 1). Three different densities were used for the volcanic edifice (2500, 2600 and 2700 kg m-3).

zero in the study area (Figure 14). We compare the observed gravity anomalies, extracted from 2-D grids (Figure 14), to anomalies, computed for the 3-D seismic model, and plotted along seismic lines R18 and R24 (Figures 6 and 12). Along line R18, the fit is good at sea, but the discrepancy increases to the NW probably due to high-density bodies intruding the crust beneath the Piton de la Fournaise [*Rançon*, 1990], which are not taken into account (Figure 6). Along line R24, the anomalies are mainly constrained by ship-borne data (Figure 14). The computed anomalies are slightly lower than the observed ones (Figure 12); nevertheless, this profile is parallel to a steep slope in the gravity anomalies along the island (Figure 14), and a small shift in the model or in the location of the observed anomalies will produce a large discrepancy.

The increase, from the basin toward the island, of the computed gravity anomalies is slightly lower than that of the observed anomalies (Figures 6 and 12). A model with a larger plate flexure, as suggested by *Bonneville et al.* [1988] and *Malengreau* [1995], would have a larger mass deficit near the island due to the thickening of the volcanic edifice, which infills the depression of the oceanic basement, and to the corresponding depression in the Moho. This will result in a further decrease in the computed anomaly and hence an increase in the misfit with the observed anomalies. There is no evidence, from the gravity anomalies, for a plate flexure larger than that inferred from seismic data.

5.5. Intermediate Velocity Material Between Crust and Mantle: Other Examples of Crustal Underplating

From the seismic detection of material with a velocity intermediate between that of normal lower crust and upper mantle, it has been proposed that a significant proportion of the products of intraplate volcanism is not erupted but rather remains intruded in the lithosphere [*Holbrook*, 1995]. Intermediate crustal seismic velocities, between 7.0 and 7.8 km/s, have been described in several environments. Beneath rifted volcanic continental margins as well as beneath oceanic islands, the top of the intermediate-velocity material coincides usually with a velocity discontinuity or with a transition zone with a strong velocity gradient [e.g., *Holbrook*, 1995; *Morgan et al.*, 1989; *Recq et al.*, 1990; *Watts et al.*, 1985], which marks the contact at the base of the preexisting crust (e.g., the prevolcanic Moho of *Caress et al.*, [1995]), with material of intermediate-velocity underplating the crust as a distinct body.

Among intraplate volcanic islands or chains investigated using exploration seismics, the existence of such underplated bodies has been discussed from diverse evidence in different situations. Early seismic investigations beneath the Hawaiian Island Chain [*Furumoto et al.*, 1973] and the island of Hawaii [*Zucca et al.*, 1982] did not show intermediate velocity material underplating the crust. *Ten Brink and Brocher* [1987], *Watts et al.* [1985], and *Watts and ten Brink* [1989] using expanding spread profiles (ESPs) together with normal incidence MCS data reported a large subcrustal body (intrusive complex) under a transect of the Hawaiian chain near the island of Oahu, where volcanic activity ceased at 2.6 Ma. However, *Lindwall* [1988], using 2-D modeling of two ESPs already interpreted by *Watts et al.* [1985], refuted the existence of a large subcrustal body. Beneath the Marquesas Archipelago, where volcanism was active from 6 to 1 Ma, evidence of crustal underplating was obtained from wide-angle seismic data recorded by OBSs and sonobuoys [*Caress et al.*, 1995]. A reflection from the middle of the thickened crust marks the top of the underplated body, equivalent to the prevolcanic base of the crust, whereas the depth to the present-day Moho is constrained by refraction within the upper mantle. In contrast, wide-angle seismic data recorded in the Canary Islands are interpreted as supporting the lack of crustal underplating, although the scarce data for the part nearest to Tenerife Island admittedly do not constrain it well [*Dalwood et al.*, 1997; *Watts et al.*, 1997].

5.6. Implications of the Shape and Size of the Underplated Body

Gallart et al. [this issue] discussed the velocity depth relation under La Réunion with respect to temperature, presence of melt, and compositional heterogeneity resulting from hotspot melt transport. The existence of the underplate and its extent are defined here along several profiles. Its shape, mapped in Figure 13, is not elongated in the SSW-NNE direction of the presumed hotspot track. The distribution of underplated material does not then appear to be controlled by the currently accepted plate drift. This is not in direct support of the discussion by *Gallart et al.* [this issue], which, assuming the commonly accepted hotspot-plate interaction model, related the spatial variation of structure derived for transect R4-R23 (Figure 2) to an evolution with time, namely, a downstream freezing of the melt in the underplated material. For the case of La Réunion, alternatives to the common view of the continuity of the hotspot supply since 65 Ma have been recently proposed. *Burke* [1996] challenges the usual interpretation of the Mascarene Ridge being the track of the Réunion hotspot emplaced since ~33 Ma [*Duncan*, 1990]. Claiming that the African Plate moved very slowly with respect to the underlying mantle since 30 Ma, he suggests that Réunion, Mauritius and Rodrigues (Figure 1) are unrelated to the Deccan hotspot which would have died under the Mascarene Ridge, and are due to young, separate hotspots [*Burke*, 1996]. Assuming the velocity of ~1.7 cm/year of *Gripp and Gordon* [1990], the location and shape of the underplated body and of La Réunion volcanic edifice itself would simply mirror that of a young La Réunion Hotspot underneath, since the displacement of the island relative to the hotspot, for the time of known volcanic activity (2.1 Ma, [*Mc Dougall*, 1971]), would be less than 40 km.

On the other hand, *Albarède et al.* [1997] noted, from the petrological study of Piton de la Fournaise and the fact that its shield-building stage does not overlap with that of Piton Des Neiges, that there is no continuity in hotspot discharge. They proposed that each volcano results from the impingement at the base of the lithosphere of what they called a blob, a solitary wave of hotspot material. They estimate its radius to be ~100 km. The underplated body, which appears similar in size, could then mark the most recent blob.

The observed limited size of the underplated body and its shape which lacks elongation could be expected in each of these models, of young hotspot, or of discontinuous hotspot discharge, to correspond then to the areal distribution of upwelling melt.

The location of the underplated body relative to the island and to the active Piton de La Fournaise appears slightly shifted southwestward (Figure 13). However, preexisting weak zones within the oceanic crust, such as the transform-fault oriented SSW-NNE under the southern coast of La Réunion discussed earlier or the fossil spreading center interpreted from magnetic anomalies to extend to the WNW of the island [*Dyment*, 1991; *Schlich*, 1982], may channel the ascending lavas between the underplated body and the active volcano (Figure 1).

5.7. Amount of Volcanic Production

The volume of the material in the crust-mantle intermediate-velocity body beneath La Réunion, inferred from this study, ranges from 30,000 to 50,000 km^3. Nevertheless, it is possible that

this body is not composed of 100% of magmatic material emplaced as a massive pluton or picritic melt but rather of preexisting upper mantle material or, in some cases, crustal material, pervaded by magmatic material through dikes and sills. Hence the actual volume of magmatic material advected at the base of the crust is necessarily overestimated by the volume of the body. The volume of volcanic material emplaced on top of the preexisting oceanic plate, between the topographic model [*Lénat and Labazuy*, 1990] and the base of the edifice, is 75,000 km^3 [*de Voogd et al.*, this issue]. Only 10,000 to 20,000 km^3 of this volume are buried beneath the average level of the oceanic basement in the small depression located southwest of the island, compared with the volume of 180,000 km^3 that would be buried in the 4 km deep (relative to the oceanic basement), 150 km radius flexural depression previously assumed [*Bonneville et al.*, 1988; *Lénat and Labazuy*, 1990].

From our estimates at La Réunion, the volume of the magmatic addition at the crust-mantle level is less than half the volume of material emplaced on top of the plate to form the volcanic edifice. For Hawaii, *Watts and ten Brink* [1989] estimated that the rate of crustal thickening due to magmatic underplating is about half the value of the rate of surface volcanic production of Kilauea. Despite difference an order of magnitude between the present effusive rate of Piton de la Fournaise, estimated at 0.3 m^3/s [*Lénat*, 1987], and that of Kilauea at 3.4 m^3/s [*Denlinger*, 1997; *Swanson*, 1972], the proportion of material underplated at the base of the crust is similar for both cases. Furthermore, there is also an order of magnitude difference between the total magmatic fluxes of the two hotspots. In their interpretation of MCS and OBS data in the Marquesas extinct hotspot archipelago, *Caress et al.* [1995] report a very large crustal underplate, which would have about twice the volume of the volcanic products deposited on top of the plate, and hence the total production of this hotspot would have been similar to the Hawaiian one, although from the amount of volcanic products extruded, it appeared significantly smaller.

If the present magmatic rate at La Réunion has been constant in the past, 8 m.y. were necessary to build the volcanic edifice, that is, only about twice the age suggested by *Bonneville et al.* [1988] and *Upton* [1982]. However, the corresponding loads and buoyancies do not produce a strong plate flexure at La Réunion, which implies different plate parameters or load densities. Consistently, the average velocity, and hence density, of the edifice on top of the plate appears different, since *Gallart et al.* [this issue] document higher velocity attributable to intrusives only under a limited part of the island and none are identified here under its submarine flanks. Comparing the velocity structure of the medium-sized Jasper seamount with the edifice of the island of Hawaii, *Hammer et al.* [1994] remarked that denser intrusives would form at most 30-50% of the volume for the seamount rising 4 km above sea bottom, whereas they are 75% of the volume for the island of Hawaii, where their thickness includes the deep depression in the preexisting plate [*Hill and Zucca*, 1987]. The relative volume of intrusives and extrusives would make La Réunion more similar to an emerged seamount than to a Hawaiian hotspot island.

6. Conclusions

Wide-angle seismic data provide velocity estimates for the gross stratification of the submarine edifice. Its upper part has a low-velocity and a strong vertical gradient, interpreted as corresponding to low-velocity, subaerially erupted, material subsequently transported underwater and subjected to compaction. Beneath the strong gradient, a layer of constant 4.5 km/s velocity is identified by a shadow zone in the wide-angle seismic data. The layer is above the base of the edifice, which is defined by the coincident MCS as the top of a low-velocity layer attributed to the underlying oceanic sediments. The no-gradient layer forming the 4.5 km/s basal unit of the edifice could be related to flows erupted underwater during the early phase before island emersion, by analogy to the velocity structure of seamounts [*Hildebrand et al.*, 1989]. Its size is difficult to estimate, since part of layer 2b just above it may be in the transition, and the profiles are not sufficiently closely spaced to map such a shallow, laterally variable unit.

On the top of the preexisting plate, wide-angle seismic data independently document several features of the oceanic basement also mapped by the coincident vertical reflection lines of *de Voogd et al.* [this issue]: a step in the underlying basement across an interpreted preexisting transform fault which is orthogonal to the south coast of La Réunion, and a landward upwarp of the oceanic basement toward the southeastern part of the island. Since the base of the crust is observed to remain flat, this basement upwarp corresponds in part to locally thicker crust. These observations support local intrusion of hotspot material into the crust under the island, since there is evidence on some coincident MCS radial lines that overlying oceanic sediments have been slightly tilted from their original horizontal stratification [*de Voogd et al.*, this issue].

An intermediate-velocity crust-mantle layer found on a transect of the island [*Gallart et al.*, this issue] is seen on several additional lines but is distinctly absent on other parts of the lines. La Réunion provides the first example we are aware of, of a tight spatial relation between a volcanically active hotspot island and an intermediate layer between the crust and mantle which appears locally introduced into the preexisting lithosphere. The magmatic addition at depth is hence coeval with, and presumably genetically related to, the active extrusive volcanism. These observations favor a model of material trapped beneath the crust, which would involve density stratification, since flexural stress cannot be invoked like in Hawaii [*ten Brink and Brocher*, 1987].

The extent of the intermediate-velocity layer may be sketched from the profiles available. It is found to thin and disappear about 80 km offshore on the radial lines in the southern half of the island. It is limited to midway under the island and definitely absent under the only available profile to the north. Hence this body extends about equally across the presumed hotspot trace as along it, with a diameter well in excess of that of the island and in excess of known eruptive centers of the whole edifice. This shape does not appear to be controlled by the commonly accepted plate/hotspot model in which *Gallart et al.* [this issue] discussed its possible interpretation as a transient feature controlled by melt fraction. The hypothesis of *Burke* [1996] that La Réunion results from the activity of a young hotspot unrelated to the track of the Deccan hotspot can account for the shape of the underplated body. Alternatively, the underplated body can result of the impingement at the base of the lithosphere of an isolated blob of hotspot material as suggested by *Albarède et al.* [1997].

The amount of hotspot material in the underplated body is less than half the volume of hotspot products on top of the plate. This proportion is similar to that estimated in the Hawaiian case, although underplating is synchronous with volcanism at La Réunion, whereas it is thought to postdate volcanism in Hawaii [*ten Brink and Brocher*, 1987].

Acknowledgments. We thank B. Toussaint (ORSTOM) and S. Operto (UMR Géosciences Azur) for their assistance in processing the data, the Groupement pour la Gestion de Navires Océanologiques, Institut Français de Recherche pour l'Exploitation de la Mer (GENAVIR–IFREMER) party (J. Hervéou, J. Le Pavec, R. Dereat, J.-C Guedès, B. Meneur, O. Quedec, and D. Vaillant) for running seismic source and MCS data acquisition flawlessly, the crew of M/V *Marion Dufresne*, B. Ollivier and Y. Balut (IFRTP), L Royer (CNRS), colleagues of the MD76 / RÉUSIS scientific party (M.D.P. Ayarza, J.J. Dañobeitia, L. Driad, G. Lelong, S. Le Roux, W. O'Brien, H. Perroud, S. Pou, D. Rousset, and M. Sachpazi), and representatives of the Mauritius Island Republic (P. O. Randamy, L. Joottun, and A. Sheik-Mamode). OBSs used during this experiment were developed and constructed by Y. Nakamura and Y. Hello at University of Texas Institute for Geophysics (UTIG). The software used for preprocessing OBS data was developed in the framework of the UTIG-ORSTOM cooperation agreement by G. Christenson, Y. Nakamura, V. Sen, M. Wiederspahn (UTIG), and B. Toussaint (ORSTOM). The MD76 / RÉUSIS cruise was financially and technically supported by IFRTP, commission de coordination de la recherche dans les départements et territoires d'outre-mer (CORDET), EEC Fournaseis project (Volcanic risk, contract EV5V-CT92-0188), and ORSTOM. T. A. Minshull acknowledge the support of the Royal Society University Research Fellowship. We thank J.-F. Lénat and P. Labazuy for their bathymetric data. Maps and model were drawn using the GMT software [*Wessel and Smith*, 1995]. We are grateful to M. Semet (IPGP) for helpful comments on an earlier version of the manuscript and to A. Levander, J. McBride, and an anonymous referee for their review of this manuscript. UMR 6526 contribution 219.

References

Albarède, F., B. Luais, G. Fitton, M. Semet, E. Kaminski, B.G.J. Upton, P. Bachèlery, and J.-L Cheminée, The geochemical regime of Piton de la Fournaise volcano (Réunion Island) during the last 530000 years, *J. Petrol.*, *38*(2), 171-201, 1997.

Bonneville, A., J.P. Barriot, and R. Bayer, Evidence from geoid data of a hot spot origin for the southern Mascarene Plateau and Mascarene Islands (Indian Ocean), *J. Geophys. Res.*, *93*, 4199-4212, 1988.

Burke, K., The African Plate, *South Afr. J. of Geol*, *99*(4), 339-408, 1996

Caress, D.W., M.K. McNutt, R.S. Detrick, and J C. Mutter, Seismic imaging of hotspot-related crustal underplating beneath the Marquesas Islands, *Nature*, *373*, 600-603, 1995.

Dalwood, R., A.B. Watts, C. Peirce, J Collier, and P Canales, Constraints on the deep structure of intra-plate oceanic islands from gravity and seismic modelling, *Terra Nova, abstr. suppl. 1*, 49, 1997.

de Voogd, B., S Pou Palomé, A. Hirn, P. Charvis, J. Gallart, D. Rousset, J. Dañobeitia, and H. Perroud, Vertical movements and material transport during hotspot activity: Seismic reflection profiling offshore La Réunion, *J. Geophys. Res.*, this issue

Denlinger, R.P., A dynamic balance between magma supply and eruption rate at Kilauea Volcano, Hawaii, *J. Geophys. Res.*, *102*, 18091-18100, 1997.

Duncan, R.A., The volcanic record of La Réunion hotspot, *Proc. Ocean Drill. Program, Sc. Results*, *115*, 3-10, 1990.

Dyment, J , Structure et évolution de la lithosphère océanique dans l'océan Indien: apport des anomalies magnétiques, thesis, 374 pp , Univ. Louis Pasteur, Strasbourg, France, 1991.

Furumoto, A.S., W.A. Wiebenga, J.P. Webb, and G.H Sutton, Crustal structure of the Hawaiian Archipelago, northern Melanesia, and the central Pacific Basin by seismic refraction methods, *Tectonophysics*, *20*, 153-164, 1973.

Gallart, J., L. Driad, P. Charvis, M. Sapin, A. Hirn, J Diaz, B. de Voogd, and M. Sachpazi, Perturbation to the lithosphere along the hotspot track of La Réunion, from an affshore-onshore seismic transect, *J. Geophys. Res.*, this issue.

Gripp, A.E., and R.G. Gordon, Current plate velocities relative to the hotspots incorporating the NUVEL-1 global plate motion model., *Geophys. Res Lett.*, *17*, 1109-1112, 1990.

Hammer, P.T.C., L.M. Dorman, J.A. Hildebrand, and B D. Cornuelle, Jasper Seamount structure: Seafloor seismic refraction tomography, *J. Geophys. Res.*, *99*, 6731-6752, 1994.

Hildebrand, J.A., L.M. Dorman, P.T.C. Hammer, A. Schreiner, and B.D. Cornuelle, Seismic tomography of Jasper Seamount, *Geophys. Res. Lett.*, *16*, 1355-1358, 1989.

Hill, D.P., and J J. Zucca, Geophysical constraints on the structure of the Kilauea and Mauna Loa volcanoes and some implications for seismomagmatic processes, *U.S. Geol. Surv. Prof. Pap.*, *1350*, 903-917, 1987.

Holbrook, W.S , Underplating over hotspots, *Nature*, *373*, 559, 1995.

Intergovernmental Oceanographic Commission (IOC), International Hydrographic Organisation (IHO), British Oceanographic Data Centre (BODC), The 1997 edition of the general oceanic chart of the oceans (GEBCO) digital atlas, Birkenhead, England, 1997.

Lankar-Bénichou, V., Approches par tomographie sismique du Piton de la Fournaise, La Réunion, thesis, Univ. Paris 7, Paris, 1997.

Lénat, J.F., Structure et dynamique internes d'un volcan basaltique intraplaque océanique: le Piton de la Fournaise (Île de La Réunion), thesis, Univ. Clermont II, Clermont-Ferrand, France, 1987.

Lénat, J.F., and P. Labazuy, Morphologies et structures sous-marines de La Réunion, in *Le Volcanisme de La Réunion*, edited by J.F. Lénat, pp. 43-74, Centre de Recherches Volcanologiques, Clermont-Ferrand, France, 1990.

Lénat, J.F., P. Vincent, and A. Bachèlery, The off-shore continuation of an active basaltic volcano: Piton de la Fournaise (Réunion Island, Indian Ocean), structural and geomorphological interpretation from SeaBeam mapping, *J. Volcanol Geotherm Res.*, *36*, 1-36, 1989.

Lindwall, D.A., A two-dimensional seismic investigation of crustal structure under the Hawaiian islands near Oahu and Kauai, *J. Geophys. Res.*, *93*, 12107-12122, 1988.

Malengreau, B., Structure profonde de La Réunion d'après les données magnétiques et gravimétriques, thesis, 366 pp , Univ. Blaise Pascal, Clermont-Ferrand, France, 1995.

McDougall, I., The geochronology and evolution of the young island of Réunion, Indian Ocean, *Geochim. Cosmochim. Acta*, *35*, 261-270, 1971.

Minshull, T.A., and J.M. Brozena, Gravity anomalies and flexure of the lithosphere at Ascension Island, *Geophys J. Int.*, *131*, 347-360, 1997.

Morgan, J.V., P.J Barton, and R S. White, The Hatton Bank continental margin, III, Structure from wide angle OBS and multichannel seismic refraction profiles, *Geophys. J. Int.*, *98*, 367-384, 1989.

Nakamura, Y., P.L. Donoho, P.H. Roper, and P. McPherson, Large-offset seismic surveying ocean-bottom seismographs and air guns: Instrumentation and field technique, *Geophysics*, *52*, 1601-1611, 1987.

Nakamura, Y , and J. Garmany, Development of upgraded ocean bottom seismograph, Univ. of Tex. Inst. for Geophys., Austin, *Technical Report*, 111 pp., 1991.

Parker, R.L., A new method for modeling marine gravity and magnetic anomalies, *J. Geophys. Res.*, *79*, 2014-2016, 1974.

Rançon, J.P., Lithostratigraphie du forage du Grand-Brûlé, implications volcanologiques, in *Le Volcanisme de La Réunion*, edited by J.F. Lénat, pp. 187-200, Centre de Recherches Volcanologiques, Clermont-Ferrand, France, 1990.

Recq, M., D. Bréfort, J. Malod, and J.-L. Veinante, The Kerguelen-Isles (southern Indian Ocean): New results on deep structure from refraction profiles, *Tectonophysics*, *182*, 227-248, 1990.

Reid, I.D., and C.E. Keen, High seismic velocities associated with reflections from within the lower oceanic crust near the continental margin of eastern Canada, *Earth Planet. Sci Lett*, *99*, 118-126, 1990.

Rousset, D., A. Bonneville, and J.F. Lénat, Detailed gravity study of the off-shore structure of Piton de la Fournaise volcano, La Réunion, *Bull. Volcanol.*, *49*, 713-722, 1987.

Sandwell, D.T., and W.H.F. Smith, Marine gravity anomaly from Geosat and ERS 1 satellite altimetry, *J. Geophys. Res.*, *102*, 10039-10054, 1997.

Schlich, R., The Indian Ocean: Aseismic ridges, spreading centers, and basins, in *The Ocean Basins and Margins, vol. 6, The Indian Ocean*, edited by A.E.M. Nairn and F.G. Stehli, pp. 51-147, Plenum, New York, 1982.

Swanson, D.A., Magma supply rate at Kilauea Volcano, *Science*, *175*, 169-170, 1972.

ten Brink, U.S., and T.M. Brocher, Multichannel seismic evidence for a subcrustal intrusive complex under Oahu and a model for Hawaiian volcanism, *J. Geophys. Res.*, *92*, 13687-13707, 1987.

Upton, B.J., The Indian Ocean: Oceanic islands, in *The Ocean Basins and Margins, vol. 6, The Indian Ocean*, edited by A.E.M. Nairn and F.G. Stehli, pp 585-648, Plenum, New York, 1982.

Watts, A.B., and U.S. ten Brink, Crustal structure, flexure and subsidence history of the Hawaiian Islands, *J. Geophys. Res.*, *94*, 10473-10500, 1989.

Watts, A.B., U.S. ten Brink, P. Buhl, and T.M. Brocher, A multichannel seismic study of lithospheric flexure across the Hawaiian Emperor seamount chain, *Nature*, *315*, 105-111, 1985

Watts, A.B , C. Peirce, J. Collier, R. Dalwood, J.P. Canales, and T.J. Henstock, A seismic study of lithospheric flexure in the vicinity of Tenerife Canary Islands, *Earth Planet. Sci. Lett.*, *146*, 431-447, 1997.

Wessel, P., A reexamination of the flexural deformation beneath the Hawaiian Islands, *J. Geophys. Res.*, *98*, 12177-12190, 1993

Wessel, P., and W.H.F. Smith, New version of the generic mapping tool released, *Eos Trans. AGU*, *76*, 329, 1995.

White, R.S., D. McKenzie, and R.K. O'Nions, Oceanic crustal thickness from seismic measurements and rare earth element inversions, *J. Geophys. Res.*, *97*, 19683-19715, 1992.

Zelt, C A., and R B. Smith, Seismic traveltime inversion for 2-D crustal velocity structure, *Geophys. J. Int.*, *108*, 16-34, 1992.

Zucca, J.J., D.P. Hill, and R.L. Kovach, Crustal structure of Mauna Loa Volcano, Hawaii, from seismic refraction and gravity data, *Bull. Seismol Soc. Am.*, *72*(5), 1535-1550, 1982.

P. Charvis, Y. Hello, A. Laesanpura, and B. Pontoise, UMR Géosciences Azur, ORSTOM, BP 48, F-06235 Villefranche-sur-Mer cedex, France. (charvis@obs-vlfr.fr)

B. De Voogd, Laboratoire de Géophysique, Université de Pau et des Pays de l'Adour, Avenue de l'Université, F-64000, Pau, France. (beatrice.devoogd@univ-pau.fr)

J. Gallart, Institut de Ciences de la Terra, C.S.I.C., Marti i Franques s/n, E-08028, Barcelona, Spain (jgallart@paleo.ija.csic.es)

A. Hirn and J.-C. Lépine, Laboratoire de Sismologie expérimentale, Insitut de Physique du Globe, Boîte 89, 4 place Jussieu, F-75252, Paris, France. (hirn@ipgp.jussieu.fr)

T. A. Minshull, Bullard Laboratoires, Department of Earth Sciences, University of Cambridge, Madingley Road, Cambridge, CB3 OEZ, England, U.K. (minshull@esc.cam.ac.uk)

(Received October 13, 1997; revised July 13, 1998; accepted August 25, 1998.)